AMERICAN SOCIETY FOR MICROBIOLOGY | Applied and Environmental Microbiology

Spotlight Selection | Bacteriology | Full-Length Text

Pantailocins: phage-derived bacteriocins from *Pantoea ananatis* and *Pantoea stewartii* subsp. *indologenes*

Shaun P. Stice,[1] Hsiao-Hsuan Jan,[1] Hsiao-Chun Chen,[1] Linda Nwosu,[1] Gi Yoon Shin,[1] Savannah Weaver,[2] Teresa Coutinho,[3] Brian H. Kvitko,[1,4] David A. Baltrus[2,5]

AUTHOR AFFILIATIONS See affiliation list on p. 12.

ABSTRACT Phage-derived bacteriocins are highly specific and effective antimicrobial molecules, which have successfully been used as prophylactic treatments to prevent phytopathogen infections. Given the specificity of tailocins, a necessary step for broadening the tailocin catalog and for extending applicability across systems and diseases is the screening of new clades of phytopathogens for the production of molecules with tailocin-like killing activity. Here, we describe the production by and sensitivity of strains to tailocins produced by *Pantoea ananatis* and *Pantoea stewartii* subsp. *indologenes*. Phylogenetic evidence suggests that these tailocins are derived from Myoviridae family phage like many previously described R-type tailocins but also suggests that cooption from phage occurred independently of previously described tailocins. Since these tailocin encoding loci are present in the same genomic locations across multiple strains of both species and display a level of divergence that is consistent with other shared regions between the genomes and with vertical inheritance of the locus, we refer to them broadly as "Pantailocins."

IMPORTANCE Phage-derived bacteriocins (tailocins) are ribosomally synthesized structures produced by bacteria in order to provide advantages against competing strains under natural conditions. Tailocins are highly specific in their target range and have proven to be effective for the prevention and/or treatment of bacterial diseases under clinical and agricultural settings. We describe the discovery and characterization of a new tailocin locus encoded within genomes of *Pantoea ananatis* and *Pantoea stewartii* subsp. *indologenes*, which may enable the development of tailocins as preventative treatments against phytopathogenic infection by these species.

KEYWORDS tailocins, phage-derived bacteriocin, *Pantoea ananatis*, *Pantoea stewartii*

The rise of antibiotic resistance across clinical and agricultural settings as well as increasing appreciation for the importance of limiting off-target effects of broad-spectrum antibiotics on beneficial microbiomes necessitates a search for new, durable, and highly specific antimicrobial compounds (1–4). Phage-derived bacteriocins, referred to as tailocins hereafter, are a class of antibacterial molecules produced by bacterial cells but originally coopted from phage tails (5–7). These molecules are released from cells by lysis to carry out killing in the extracellular environment, maintain high efficiency and specificity in killing of target cells, and have been shown to be effective in preventing infection of plants by phytopathogens (8, 9). Here, we sought to expand the arsenal of known tailocins and identify new types of tailocin molecules that could be used as prophylactic agricultural antibacterials by screening for production and sensitivity across strains of genus *Pantoea* which include several phytopathogens.

Tailocins are antibacterial compounds that closely resemble active phage, except that they largely consist of phage tail proteins (sheath, spike, tail fibers) and, therefore, lack

Editor Gladys Alexandre, University of Tennessee at Knoxville, Knoxville, Tennessee, USA

Address correspondence to David A. Baltrus, baltrus@email.arizona.edu.

The authors declare no conflict of interest.

See the funding table on p. 13.

See the companion article at https://doi.org/10.1128/MRA.00471-23.

Received 2 June 2023
Accepted 15 September 2023
Published 20 November 2023

most if not all proteins involved in capsid production and phage replication (7). Pathways for tailocin production are encoded within the bacterial genome, with an individual cell producing hundreds of these structures before they are released to the environment through cell lysis (6, 7, 10). Tailocins are highly efficient in their killing activity, with this lethal activity thought to be due to mechanical disruption of membrane integrity when the spike protein penetrates membranes of sensitive cells (5, 11). Binding of tailocins to target cells has been shown thus far to be primarily controlled by sequence variation in tail fiber proteins and associated chaperones, which are thought to interact with sugar moieties in the lipopolysaccharide (LPS) of target cells in all systems where binding has been characterized (12–16). Unlike other bacteriocins, tailocin loci do not encode their own resistance loci, and cells are protected from self-killing through modification of their LPS through addition or recombination of LPS-modifying genes at other locations in the genome (13, 16, 17). As with all bacteriocins, tailocins are thought to largely target closely related strains to the producer cells, although tailocins from a handful of strains have been shown to possess a broader target range (18, 19). Given these properties, tailocins display incredible potential for development as next-generation antimicrobials, with our group and others already demonstrating that tailocins can be applied to plants as a prophylactic treatment to prevent infection by phytopathogens (8, 9).

Much of our knowledge concerning tailocins comes from a number of *Pseudomonas* species that produce a variety of tailocin molecules that appear to have independently evolved from different progenitor phage (20). Specifically, *Pseudomonas aeruginosa* can produce two distinct tailocins, which are referred to as R-type pyocins (which possess a rigid contractile tail) and F-type pyocins (which possess flexible tails) (6, 7). R-type pyocins are considered by many to be the canonical tailocin, is closely related to the Myoviridae phage P2, and has been the focus of research for numerous decades (7, 11, 21). Our group has also demonstrated that *Pseudomonas syringae* produces an R-type syringacin which we showed to have evolved independently from R-type pyocins and which is more closely related to the Myoviridae phage Mu than P2 (22). Close evolutionary relationships between extant phage and tailocins render it difficult to definitively identify tailocins by genome sequence alone when evaluating loci in the context of "incomplete" phage regions. Despite such challenges, there have been an increasing number of tailocin-producing strains identified, with producers spanning a range of bacterial genera including both Gram-negative and Gram-positive cells and including multiple lineages classified as Enterobacterales (10, 23–26). In one case, *Erwinia* strain Er (now identified as *Pectobacterium carotovorum*) was shown to have the capacity to attach different tail fibers to the tailocin structure, with an invertible region determining which specific tail fiber was encoded by this genome (27).

Given the demonstrated production of tailocins by other Enterobacterales, we sought to screen for tailocin-like killing activity from a variety of *Pantoea* strains isolated from plants. Here, we report that multiple strains within this genus have the genetic capacity to produce tailocins and that loci encoding these tailocins maintain at least two distinct killing spectra. Tailocin loci from both species are relatively closely related to each other and are likely derived from a common ancestral locus but are also closely related to extant phage found across Enterobacterales strains and species.

MATERIALS AND METHODS

Screening *Pantoea* strains for tailocin production

All strains and other genetic materials used in the manuscript are listed in Table 1 (28–34). We first screened for tailocin-like killing activity against *P. ananatis* strain PNA 97-1R using soft agar overlays, which are described below and as well as in a previous publication (35).

Supernatants used in this screen were induced for tailocin production and isolated from strains *P. allii* PNA 200-10, *P. agglomerans* PNG 92-11, *P. agglomerans* PNG 97-1, *P. ananatis* ATCC 35400, *P. stewartia* subsp. *indologenes* 0696-21, and *P. stewartii*

TABLE 1 Genetic/genomic resources

Cultured bacteria				
Species and strain (alternate designation)	**Baltrus lab number**	**Origin and/or features**	**GenBank assembly accession**	**Source/citation**
P. ananatis PNA 97-1R		Onion, GA USA	ASM295203v2	(28)
P. ananatis ATCC 35400 (X9)	DBL1721	Honeydew melon, CA USA	ASM2943391v1	(29)
P.allii PNA 200-10		Onion, GA USA	ASM314893v1	(30)
P. agglomerans PNG 97-1		Onion, GA USA	ASM436890v1	(30)
P. agglomerans PNG 92-11		Onion, GA USA	ASM314900v1	(30)
P. stewartii subsp. *indologenes* 0696-21		Sudan grass, CA USA	N/A	(31)
P. stewartii subsp. *indologenes* ICMP 10132 (IBSBF 731)	DBL1720	Sugarcane, Brazil	ASM2943396v1	(32)
P. ananatis ATCC 35400 Δtail::cat	DBL1826	Tailocin deletion, CmR		This study
P. stewartii subsp. *indologenes* ICMP 10, 132R1 Δtail::cat	DBL1818	Spontaneous RfR isolate, tailocin deletion, CmR		This study
E. coli RHO5		SM10 derivative RP4/RK2 conjugation strain, DAP auxotroph, pir116+ for replication of pir-dependent R6K plasmids		(33)
Additional bacterial genomes				
Species and strain (alternate designation)			**GenBank assembly accession**	
P. ananatis PNA 99-7			NMZW01000000.1	
P. ananatis MMB-1			JAABOW000000000.1	
P. ananatis NFR11			FPJM01000000.1	
P. ananatis Lstri			CP060818.1	
P. stewartii subsp. *indologenes* ZJ-GFZX1			CP049115.1	
P. stewartii subsp. *stewartii* DC283			CP017581.1	
P. stewartii subsp. *indologenes* HR3-48			CP099540.1	
P. stewartii M073a			JSXF01000000.1	
P. stewartii subsp. *indologenes* LMG 2632			JPKO00000000.1	
Plasmids				
Plasmid name	**Plasmid features**			
pR6KT2G	Gateway BP clonase II compatible R6K-based allelic exchange vector derived from pR6KT2, GmR, gus+, sacB, CmR (Gateway cassette)			(34)
pR6KT2G::Δtail1_ATCC35400	Cat marked allelic exchange deletion of P4908_16535 to P4908_16555; GmR, CmR			This study
pR6KT2G::Δtail1_ICMP10132	Cat marked allelic exchange deletion of P4910_13665 to P4910_13685; GmR CmR			This study

subsp. *indologenes* ICMP 10132 (which was originally identified as *P. ananatis*, but the isolate within our strain collection has been subsequently identified as a member of *Pantoea stewartii* subsp. *indologenes* based on whole genome sequencing, ANI (average nucleotide identity) analysis, and subspecies-specific PCR as described in the companion manuscript https://doi.org/10.1128/MRA.00471-23). We then screened for tailocin production of the same strains against *P. ananatis* strain ATCC 35400. For preparation of tailocins, methods were slightly adapted from previously described reports (35). Briefly, single colonies of each strain were grown overnight in lysogeny broth (LB) media at 27°C. Each culture was then back diluted 1:100 in LB media and grown for 4 hours while shaking at 27°C, at which point mitomycin C was added to each culture to a final concentration of 0.5 µg/mL. The next day, tailocins were isolated using PEG precipitation and stored for overlay experiments.

For overlay experiments, single colonies of each strain were grown overnight in LB media at 27°C. Each culture was then back diluted 1:100 in LB media and grown for 4 hours. After 4 hours, 100 µL of each culture was added to 3-mL molten 1.5% water agar

and poured onto LB agar plates, and the top agar was allowed to solidify for ~15 minutes. At this point, a fivefold dilution series was prepared for each tailocin in PEG buffer, after which 10 µL of the tailocin preparations was added to the overlay plate. Plates were incubated at 27°C for 1 day at which point plates were observed for tailocin-like killing activity.

Transmission electron microscopy of potential tailocins

In all cases, cultures were prepared and PEG precipitated as above to induce and purify tailocins, and then these treatments were visualized using transmission electron microscopy as per reference (22). Briefly, supernatants from cultures of wild-type (DBL1720, DBL1721) and structural mutants (DBL1818, DBL1826) were prepared from strains *P. stewartii* subsp. *indologenes* ICMP 10132 and *P. ananatis* ATCC 35400, respectively. Cultures were induced for tailocin production and then concentrated and purified by PEG precipitation. Four microliters of concentrated tailocin samples were placed on glow-discharged, carbon-coated grids (Formvar-carbon, 200 mesh copper) for 5 minutes and then partially blotted to ~1 µL. Grids were rinsed twice on ddH2O droplet for 5 minutes. Two percent aqueous uranyl acetate was applied on grids for negative staining. Grids were visualized on a JEOL JEM1011 (JEOL USA, Inc., Peabody, MA) transmission electron microscope (TEM) operated at 100 kV at the Georgia Electron Microscopy, University of Georgia. Images were taken with a high-contrast 2k × 2k AMT mid-mount digital camera at 50,000× magnification.

Genome sequencing of *P. ananatis* ATCC 35400 and *P. stewartii* subsp. *indologenes* ICMP 10132

Draft genome sequences were generated for one strain from each *Pantoea* tailocin class, with details of genome sequencing and assembly described in the companion manuscript. For *P. stewartii* subsp. *indologenes* ICMP 10132, the Whole Genome Shotgun project has been deposited at DDBJ/ENA/GenBank under the accession JARNMT000000000. The version described in this paper is version JARNMT010000000. For *P. ananatis* ATCC 35400, the Whole Genome Shotgun project has been deposited at DDBJ/ENA/GenBank under the accession JARNMU000000000. The version described in this paper is version JARNMU010000000.

Identification of tailocin locus from two different strains

Each genome sequence was queried for potential phage regions using PHASTER (36), and regions that did not appear to code for complete prophage upon manual inspection were further analyzed. Manual inspection of genomes for both ICMP 10132 and ATCC 35400 highlighted that there exists one potential region in each genome identified as a prophage but which apparently lacks capsid production and phage replication genes and which was therefore consistent with production of a tailocin. Neither of these regions displayed close sequence similarity to previously described tailocins (Fig. 5). We provide locus numbers and annotations for genes found within the tailocin locus from the publicly annotated version each genome in Table 2.

Deletion of tailocin structural loci from each strain

For each strain, allelic exchange constructs were designed to disrupt a large portion of the predicted tailocin region by targeting five genes predicted to encode tail fibers and baseplate proteins (Fig. 2). Allelic exchange in *Pantoea* strains was conducted as described by Stice et al. (34). Briefly, 400-bp regions flanking the desired deletion were directly synthesized as dsDNA upstream and downstream of the cat chloramphenicol resistance gene and promoter by GenScript. Synthesized DNA was recombined using BP clonase II into the conditional allelic exchange vector pR6KT2G. Conjugation with the DAP auxotrophic biparental mating strain *E. coli* RHO5 was used to deliver the allelic exchange vectors. Single cross-over merodiploids were recovered by selection

TABLE 2 Tailocin protein loci and current annotations

ICMP 10132 locus	ATCC 35400 locus	Annotation
	P4908_16470	Tyrosine recombinase
	P4908_16475	Hypothetical
P4910_13590	P4908_16480	Toxin-antitoxin hicB
P4910_13595	P4908_16485	Hypothetical
P4910_13600	P4908_16490	ogr/delta-like zinc finger family protein
P4910_13605	P4908_16495	VgrG/Pvc8 family
P4910_13610	P4908_16500	Phage tail protein gpU family
P4910_13615	P4908_16505	Phage tape measure protein
P4910_13620	P4908_16510	Phage tail assembly protein GpE
P4910_13625	P4908_16515	Hypothetical
P4910_13630	P4908_16520	Tail tube protein
P4910_13635	P4908_16525	Tail sheath protein gpFI
P4910_13640	NA	YciL family
P4910_13645	NA	Inverase Hin family
NA	P4908_16530	Tail fiber assembly protein
P4910_13650	NA	Tail fiber assembly protein
P4910_13655	NA	Hypothetical
P4910_13660	NA	Hypothetical
P4910_13665	P4908_16535	Tail fiber protein
P4910_13670	P4908_16540	Phage tail protein I
P4910_13675	P4908_16545	Baseplate assembly protein J
P4910_13680	P4908_16550	GPW/gp25 family protein
P4910_13685	P4908_16555	Baseplate assembly protein V
P4910_13690	P4908_16560	Tail completion protein R (GpR)
P4910_13695	P4908_16565	LysC
P4910_13700	P4908_16570	LysB
P4910_13705	P4908_16575	Lysozyme
P4910_13710	P4908_16580	HP1 family holin
P4910_13715	P4908_16585	Tail protein X
P4910_13720	P4908_16590	Tum (DinI family protein)
P4910_13725	P4908_16595	Replication endonuclease
P4910_13730	P4908_16600	TraR/DksA C4 type zinc finger protein
P4910_13735	P4908_16605	DUF2732
P4910_13740	P4908_16610	hypothetical
P4910_13745	P4908_16615	Ci phage repressor

on gentamicin and chloramphenicol, and double cross-over deletion strains were subsequently recovered by sucrose counter-selection and chloramphenicol selection with screening for loss of the *uidA* color marker on X-gluc and gentamicin sensitivity. Deletions were confirmed by PCR genotyping with independent primers designed to anneal outside the deletion flanks. Tailocin mutant strains were tested for loss of tailocin killing in an overlay assay as well as loss of visible tailocin-like structures by TEM as described above (see supplemental data and figures at doi.org/10.6084/m9.figshare.22596982.v1).

Phylogenetic methods

Protein sequences for the baseplate J protein (gp47) and sheath protein from *P. ananatis* ATCC 35400 and *P. stewartii* subsp. *indologenes* ICMP 10132 were used to query the GenBank nr database with BlastP to find sequences with high similarity from other Enterobacterales species. Protein sequences from these loci were also sampled from multiple *P. ananatis* and *P. stewartii* species that possessed either complete genome sequences or where the *rpoD* to *fadH* locus was contiguous in draft genome sequences.

Presumably homologous sequences were sampled from genomes of strains with previously characterized tailocins and similar phage including *P. aeruginosa* PA01 and P2, *P. syringae* pv. *syringae* B728a and Mu, *Pectobacterium carotovorum* strains Er (baseplate) and WPP14 (sheath), *P. putida* BWMM1, *P. fluorescens* A506, *Kosakonia* DSM16656, *Xenorhabdus boveinii* SS-2004, and *Photorhabdus luminescens* subsp. *laumondii* TTO1. Lastly, where identification was possible, J protein and sheath sequences were sampled from additional prophage in *P. ananatis* and *P. stewartii* strains found contiguous with Pantailocin loci in the region between *rpoD* and *fadH*.

Protein sequences were aligned using Clustal Omega with default parameters (37). Alignments were queried in Modeltest to find the most appropriate evolutionary model for inferring maximum likelihood phylogenies (38). RAxML-ng was used to infer phylogenies for each protein alignment, with the LG + G4 + F model used for inference for both alignments (39). Bootstrapping was performed for each alignment and carried out until models converged according to tests within RAxML-ng. Bootstrapping scores were placed on the best tree for each alignment using the Transfer Bootstrap Expectation calculation in RAxML-ng.

RESULTS AND DISCUSSION

Identification of tailocins from *Pantoea* strains

Multiple strains classified as Enterobacterales have been shown to possess the ability to produce phage-derived bacteriocins (also known as tailocins), but such molecules have not previously been characterized from *Pantoea* species (10). We find tailocin-like killing activity when supernatant preparations from *P. ananatis* strain ATCC 35400 are tested against *P. ananatis* PNA 97-1R but not from supernatants from a selection of other strains and species (Fig. 1A). This activity forms a crisp border in the overlay assay and does not form single plaques upon dilution, characteristics which are consistent with tailocin-based killing in other systems. We next tested supernatant preparations from each of these strains in overlay assays using ATCC 35400 as the indicator strain. These assays demonstrated that preparations from *P. stewartii* subsp. *indologenes* strains 0696-21 and ICMP 10132 also possess tailocin-like killing activity (Fig. 1B) suggesting the presence of a tailocin locus in these strains. Given these results, we independently isolated new tailocin preparations from strains ATCC 35400 and ICMP 10132 and visualized these preparations by transmission electron microscopy. In both cases, visualization of these preparations displayed tailocin-like structures which resemble Myoviridae phage but which lack a capsid (Fig. 2A and B). Within our preparations, there are also numerous examples of tailocin molecules that have already fired as well as those which appear as empty sheath molecules. Since we have shown that these tailocins are found in both *Pantoea ananatis* and *Pantoea stewartii* and that at least a portion of the killing is cross-species, we refer to these tailocins as "Pantailocins."

Upon generating draft genome sequences for both ATCC 35400 and ICMP 10132, we searched for potential tailocin encoding loci by first identifying phage regions using PHASTER (36) and manually screening these regions for genomic characteristics consistent with encoding tailocins instead of phage. Predicted tailocins for each strain were found in a region bordered by *dnaG* and *rpoD* as well as a tRNA locus for methionine on one side and by lipoprotein E and *fadH* on the other side. This region in ATCC 35400 appears to contain one predicted tailocin as well as an operon that is predicted to encode proteins involved in nutrient transport. In ICMP 10132, this region appears to encode an additional phage or phage-like structure but lacks genes related to nutrient transport. The conserved border regions (*dnaG/rpoD* and lipoprotein/*fadH*) for the two strains share 80%–90% nucleotide similarity, which is roughly the same divergence as most loci predicted to encode tailocins found in both strains (Fig. 3). The main difference in alignment of the tailocin regions involves predicted tail fibers, which have been shown to be critical for host targeting specificity of tailocins in other systems. In ATCC 35400, the tail fiber is predicted to be encoded by genes for a receptor binding protein and an associated chaperone. In other systems and in phage, this chaperone protein aids in

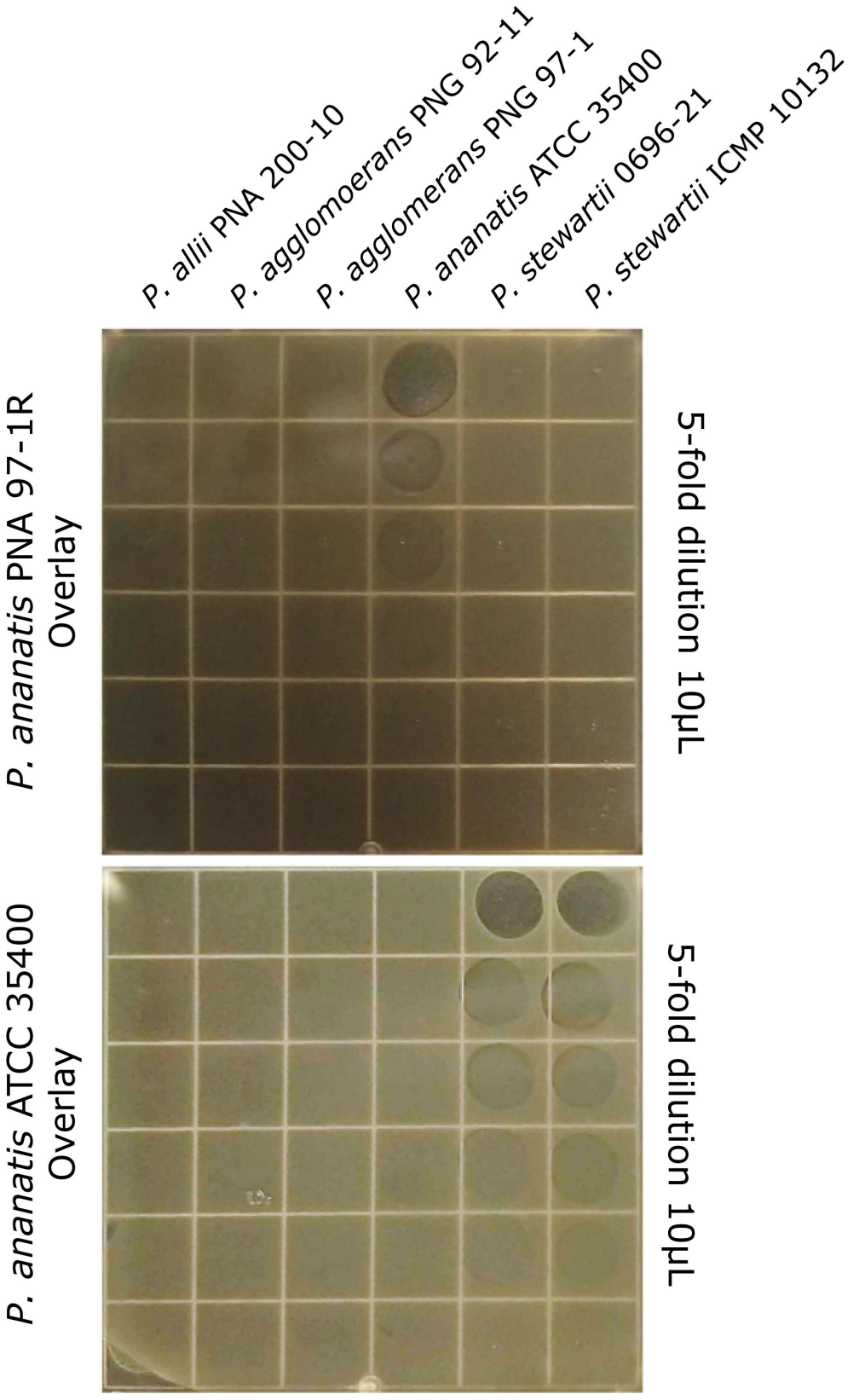

FIG 1 *Pantoea* strains display tailocin-like killing activity. A selection of *Pantoea* strains were tested for the ability to produce tailocin-like killing activity against *P. ananatis* PNA 97-1R (top) and *P. ananatis* ATCC 35400 (bottom). Columns represent antimicrobial activity of preparations from each strain against either of the two target strains, while rows indicate a fivefold dilution series of the tailocin preparations.

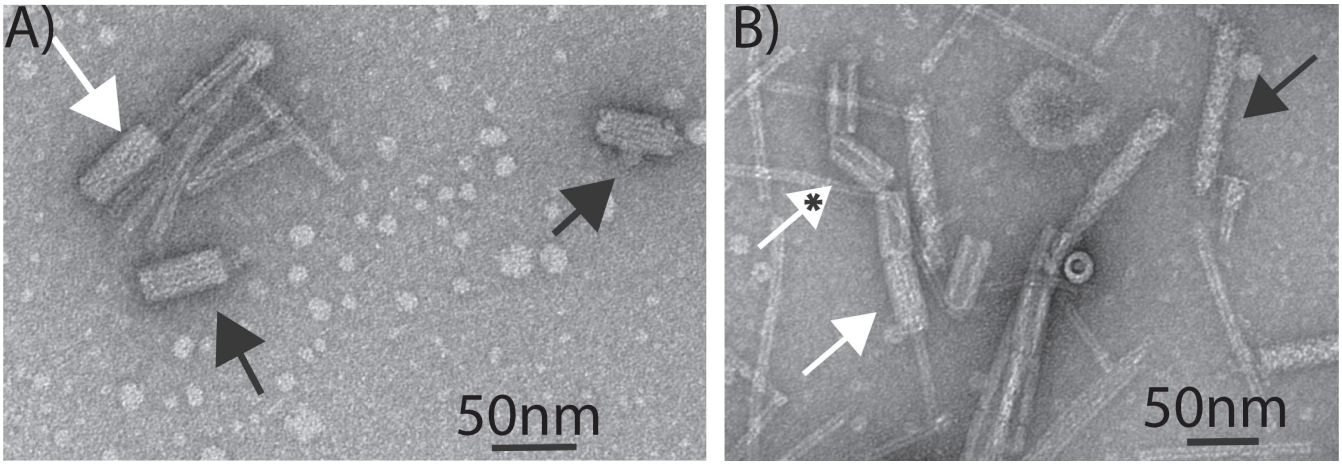

FIG 2 Tailocin-like molecules produced by *Pantoea* strains. We evaluated the production of tailocin molecules by strain (A) ATCC 35400 and (B) ICMP 10132 using transmission electron microscopy (TEM). Shown are two representative pictures from these TEM preparations. Black arrows indicate tailocins that appear to be ready to fire (or which have already fired and have broken the tail tube during preparation), while white arrows potentially represent tailocin sheaths that have already fired. We include a white arrow with an asterisk to indicate an empty sheath. Original images and additional images can be found at doi.org/10.6084/m9.figshare.22596982.v1.

attachment of the tail fiber to the rest of the phage tail complex but may also be involved in attachment to target cells (40, 41). The tail fiber region in ICMP 10132 is highly diverged from that in ATCC 35400 and stands out from the rest of the predicted tailocin locus because there is little to no nucleotide similarity in these genes between the two strains (Fig. 3). Such a level of divergence is suggestive of localized recombination and horizontal transfer of tail fiber genes for these tailocins as has been demonstrated in *P. syringae* tailocins (14). Strikingly, the recombination point in *Pantoea* appears to be anchored in the N terminus of the tail fiber gene, which was also shown for *P. syringae* tailocins. We also note that, in ICMP 10132, there is a gene predicted to encode an invertase immediately adjacent to the receptor binding protein (Rbp) and chaperone. Translation of nucleotide sequences between the invertase and Rbp/chaperone suggests that this locus could encode the C-terminus of an additional Rbp as well as an additional chaperone, which highlights potential for strain ICMP 10132 to alternate tailocin targeting through an invertase-based switch. We present a potential model for how this invertase switch functions as Fig. S1.

Deletions within predicted tailocin regions abolishes killing activity

To test for associations between these predicted regions and tailocin-like killing activity, we generated multi-gene deletions within predicted tailocin regions for strains ATCC 35400 and ICMP 10132. Specifically, we intended to delete matching stretches of tailocin

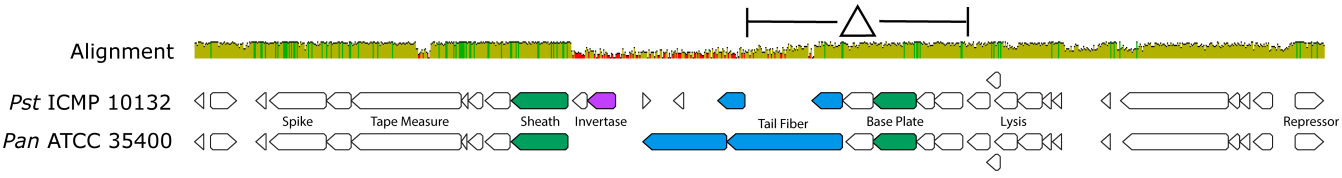

FIG 3 A schematic of Pantailocin encoding loci. Nucleotide sequences from tailocin regions for *Pst*ICMP 10132 and *Pan*ATCC 35400 were aligned against each other, and the alignment and predicted ORFs within each tailocin locus are shown. Nucleotide similarity is displayed by both the height of the alignment similarity bar as well as the colors within the bar itself (green, >80% similarity; yellow, 40%–80% similarity; red, <40% similarity). Loci encoding major tailocin genes for both strains are labeled, and the region that was deleted in each strain to create tailocin mutants is also shown. Image originally created in Geneious Prime 2020.2.4 (https://www.geneious.com) and modified thereafter. Potential tail fiber proteins and their chaperones are colored blue, the potential invertase is colored purple, loci used to infer phylogenetic relationships are colored green, and all other predicted genes are shown in white.

structural genes in each strain background, and we were able to isolate independent strains with syntenic regions deleted in both ATCC 35400 and ICMP 10132. In each case, deletions eliminated tailocin-like killing activity present in the wild-type strains when evaluated using overlay assays (Fig. 4). We have also visualized preparations from these deletion strains using TEM and as part of the same preparations used to visualize the wild-type strains as above and note that there are few (if any) tailocin-like structures created in these deletion mutants (see supplemental data and figures at doi.org/10.6084/m9.figshare.22596982.v1).

Tailocin loci are predicted to be found in additional *P. ananatis* and *P. stewartii* strains

To gauge the distribution of potential tailocin loci across both *P. ananatis* and *P. stewartii*, we investigated the region in between *rpoD* and *fadH* in closed genomes for multiple strains of each species (Table 1) with a focus on strains with complete genome sequences where the entirety of this region was contiguous. In many strains, we found evidence for independent prophage integration at this site, similar to what is found in ICMP 10132, as well as a relatively high level of presence/absence diversity in genes between *rpoD* and the predicted start of the tailocin loci. However, we did find evidence for Pantailocin encoding loci similar to those described for ATCC 35400 and ICMP 10132 in this region of every genome of *P. ananatis* investigated and in a majority of genomes classified as *P. stewartii* subsp. *indologenes*. The only analyzed *P. stewartii* genome that appeared to lack a tailocin locus between *rpoD* and *fadH* was DC283, which is a reference strain used to study virulence in *P. stewartii* subsp. *stewartii*. As a further comparison of tailocin loci, we aligned regions spanning from the tailocin tape measure protein through baseplate protein V (Fig. 5). As shown in Fig. 3 for ATCC 35400 and ICMP 10132, tailocin regions align quite well across *P. ananatis* and *P. stewartii* strains except for extensive diversity in the loci coding for predicted receptor binding proteins (Fig. 5). Moreover, many of

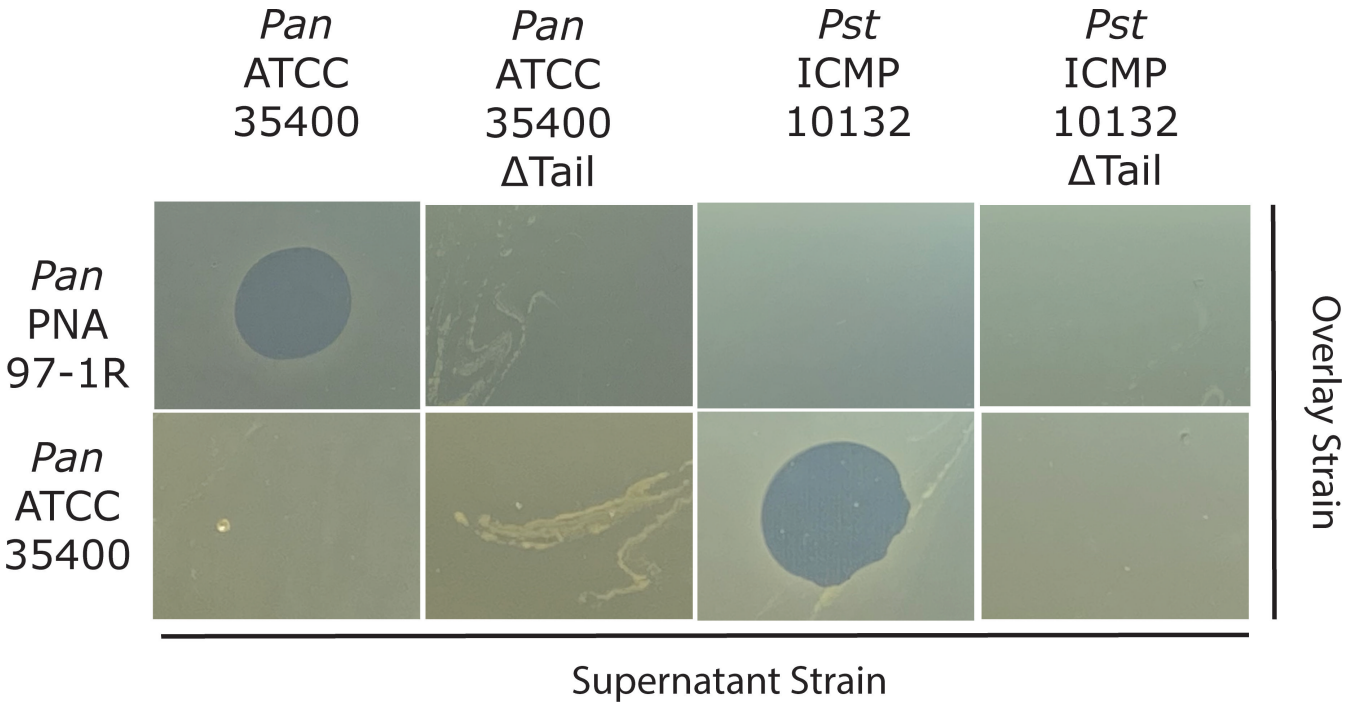

FIG 4 Deletion of tailocin structural genes abolishes killing activity for both strains. We created mutants for each strain whereby multiple tailocin structural genes were deleted (see Fig. 3). Tailocin preparations for both wild-type and mutant strains were then overlaid onto the two original target strains (PNA 97-1R and ATCC 35400). Tailocin-like activity is demonstrated by clear and crisp killing zones by each strain against its original target and is abolished in each mutant. Original images can be found at doi.org/10.6084/m9.figshare.22596982.v1.

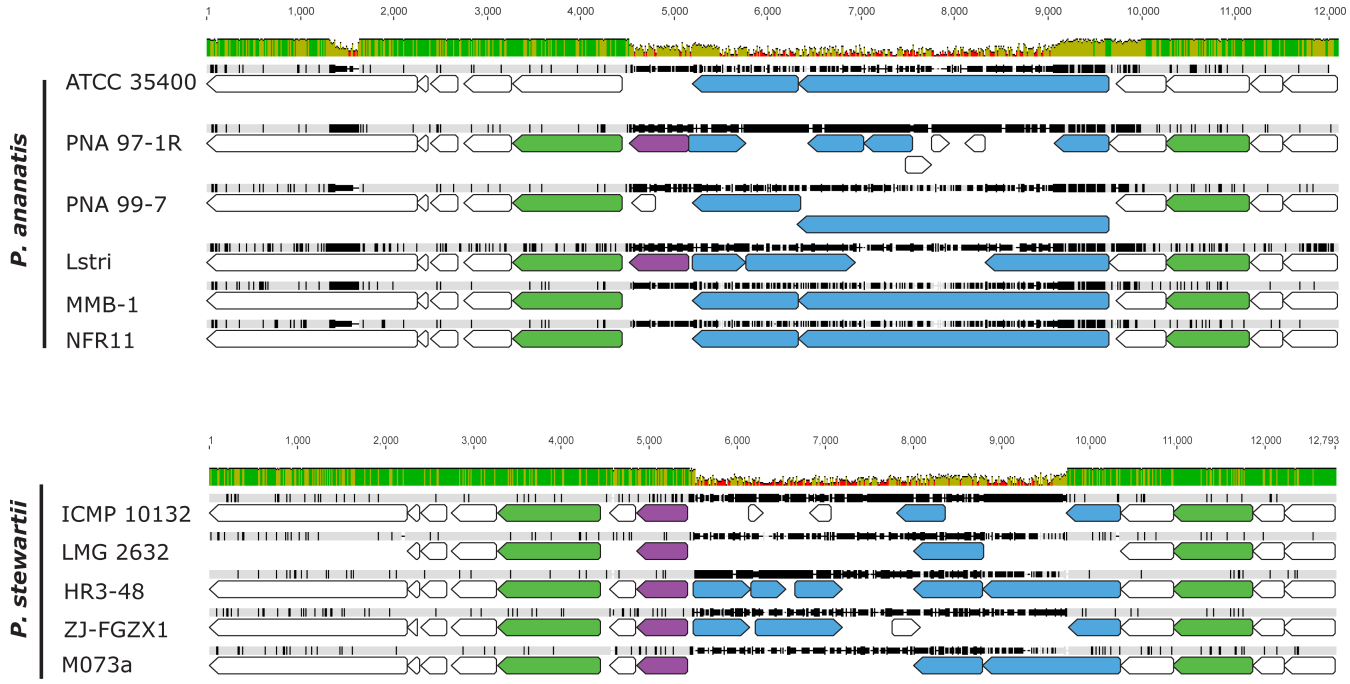

FIG 5 Alignment of Pantailocin loci across *P. ananatis* and *P. stewartii* strains. Nucleotide sequences for regions spanning the tape measure protein to baseplate protein V from predicted tailocin regions for numerous *P. ananatis* and *P. stewartii* strains were aligned, and the alignment and predicted ORFs within each tailocin locus are shown. Nucleotide similarity is displayed by both the height of the alignment similarity bar as well as the colors within the bar itself (green, >80% similarity; yellow, 40%–80% similarity; red, <40% similarity). Potential tail fiber proteins and their chaperones are colored blue, the potential invertase is colored purple, and all other predicted tailocin genes are shown in white. Loci used to infer phylogenetic relationships are colored green. Image originally created in Geneious Prime 2020.2.4 (https://www.geneious.com) and modified thereafter. Original alignments and phylogenetic data can be found at https://doi.org/10.6084/m9.figshare.22596982.v1.

the examined tailocin loci across *P. ananatis* strains and all *P. stewartii* strains including the confirmed ICMP 10132 Pantailocin appear to encode an invertase that presumably enables inversion within the tailocin region. Such a molecular switch could impart in the genetic capability for strains containing this invertase to encode multiple tail fibers with different specificities.

Pantoea tailocin loci are divergent from previously described tailocins

R-type tailocins have been described from a diverse range of bacteria, from Gram-positive genera like *Listeria* and *Clostridium* to numerous Gram-negative species (17, 19, 20, 23–26, 42–46). While the best characterized tailocin loci to date are the R pyocins of *P. aeruginosa* and the R syringacins of *P. syringae*, numerous examples of tailocin encoding loci have been described throughout *Enterobacteraceae* (10, 24–27). In each case, it appears as though tailocin loci have been coopted from Myoviridae phage progenitors, with cooption involving loss of capsid, replication, and cargo genes from these phage but with retention of main structural components of the tail as well as lysis enzymes enabling release of tailocins from the cell (6, 7).

Comparisons across tailocin loci also demonstrate that, although tailocin production is often induced by DNA damage, the complexity of regulatory pathways controlling tailocin operons often diverges between tailocin operons and can involve different suites of genes as well as divergent regulatory links to additional cellular processes (22, 47, 48). For instance, *Pseudomonas* tailocins are controlled by the actions of both a LexA-like repressor (called PrtR in *P. aeruginosa*) which is encoded next to a positive regulator (PrtN in *P. aeruginosa*) (22, 47). The *Pantoea* tailocin loci each contain a LexA-like negative regulator, found two loci away from a potential positive regulator (TraR/DksA-like zinc finger protein), but also potentially encode a Tum-like (DinI family) protein that could

interact with LexA-like repressor (Table 2). Tailocins and bacteriocins are often induced using DNA damaging agents like mitomycin C under laboratory conditions, and it is likely that DNA damage from competition and/or environmental stress can trigger expression of tailocin loci in nature (35, 49). However, an additional recent report demonstrated that tailocins in *P. syringae* were induced during "normal" conditions of infection *in planta* and in the absence of induction of additional pathways (and phage) that are responsive to DNA damage (50). Therefore, it is possible that expression from the tailocin locus is fine tuned under natural conditions and moderated by interactions between levels of DNA damage as well as secondary environmental signals.

To better understand the evolutionary relationships between tailocin loci encoded by *Pantoea* and those described from other systems, we inferred phylogenies for predicted baseplate protein (J-like, gp47) alleles as well as the predicted sheath proteins encoded by these systems, by related phage, and by other described tailocin systems. Phylogenies for both proteins show consistent relationships between alleles of the proteins investigated with strong bootstrap support for many of the major clades and divisions. The tailocin baseplate and sheath proteins from *Pantoea* strains ATCC 35400 and ICMP 10132 form clades with predicted Pantailocin loci from closely related strains within the same species. Together, loci from *Pantoea* tailocins form a single clade to the exclusion of proteins from other tailocins: including the R pyocin from *P. aeruginosa*, R syringocin from *P. syringae*, and the previously described *Pectobacterium* R carotovoricin as well as all other known tailocin loci. Moreover, loci from *Pantoea* tailocins are more closely related to those from *Erwinia* phage ENT90 than to either phage P2 or to other sampled tailocin loci.

Previously described tailocin loci from *Pseudomonas aeruginosa*, *Pseudomonas fluorescens*, *Pseudomonas putida*, and *Pseudomonas syringae* appear to have independently arisen through cooption of different progenitor phage from the Myoviridae family. In the case of *P. aeruginosa*, the most well-described closely related phage to R-type

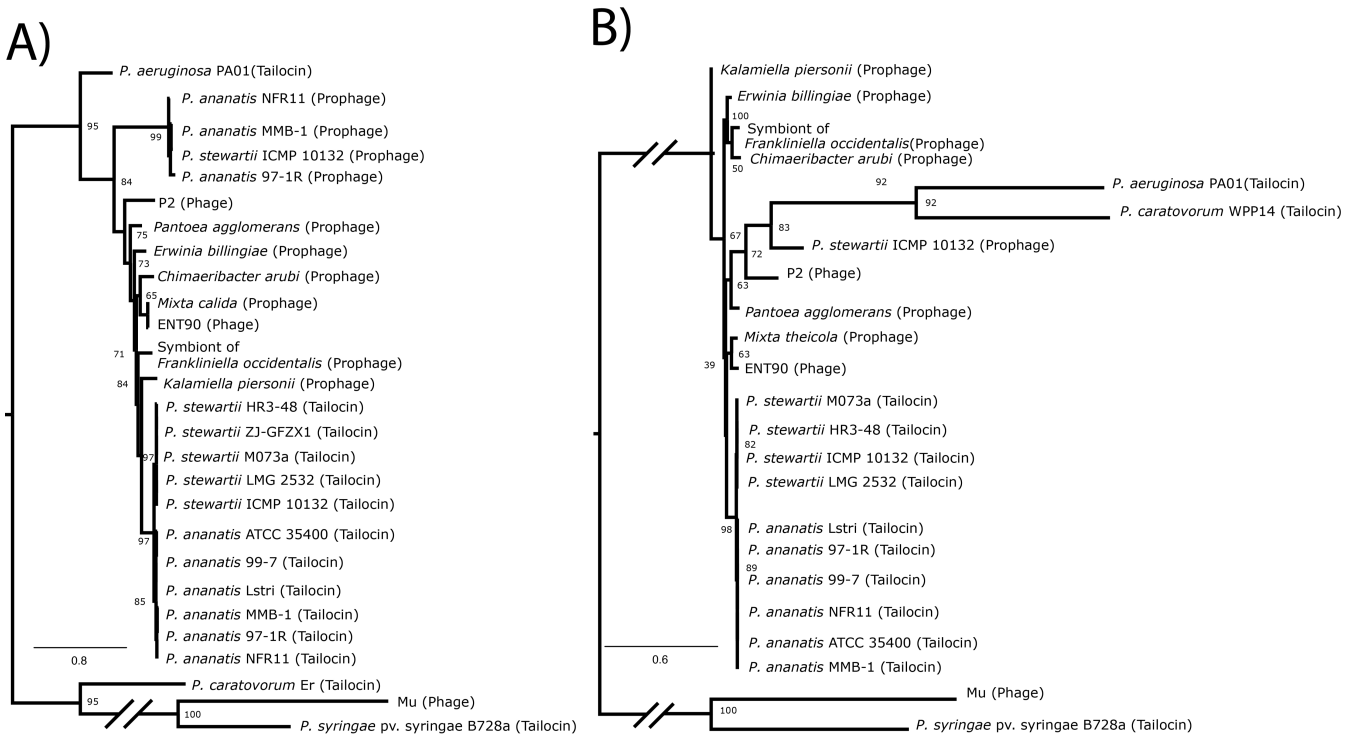

FIG 6 Phylogenetic relationships of Pantailocin loci compared to other phage and tailocins. Maximum likelihood phylogenies for the (A) J plate and (B) sheath protein were inferred using alignments from predicted and known tailocins as well as related phage and prophage. Bootstrap values are shown for major nodes, but when not shown, bootstrap values are generally <75 (e.g., in the *P. ananatis* and *P. stewartii* tailocin clades where there is little resolution to determine phylogenetic relationships).

pyocins is P2 (21), while the most well-described closely related phage to R-type syringacins is Mu (22). Phylogenetic relationships suggest that, like the R-type pyocins of *P. aeruginosa*, tailocins from *Pantoea* are derived from a phage that resembles P2 rather than Mu but also that this may also represent an independent cooption of phage into tailocins given close relationships with extant phage to the exclusion of proteins from phage P2 as well as the R-type pyocins. Indeed, inspection of these phylogenies highlights that most tailocin loci from different species and genera are relatively divergent from each other (with the exception of *Xenorhabdus/Photorhabdus*). Therefore, there is a strong possibility that many of the tailocin loci found in different genera and species are products of independent phage cooption events and that cooption of prophage into tailocins occurs quite readily over evolutionary time. However, definitive characterization of potential origins of Pantailocins and of tailocin loci in general will require additional extensive sampling of bacterial and phage genomes and additional evolutionary analyses as it is also possible that recombination between tailocins and extant phage is obscuring definitive evolutionary signals.

We also note that even though a tailocin containing an invertase switch has previously been shown for carotovoricin Er (27), a tailocin encoded by *Pectobacterium carotovorum*, the predicted tailocin in ICMP 10132 is highly divergent to the previously described locus from *Erwinia* strain Er (Fig. 6) and that the *Pectobacterium* tailocin is more close in sequence to *P. aeruginosa* R-type pyocins than the *Pantoea* tailocins described here. Therefore, tailocins from *Pantoea* and from *Pectobacterium* and their invertible tail fibers also appear to have independently arisen from divergent ancestor phage.

Conclusions

We have described new tailocin loci found within the genomes for strains characterized as both *Pantoea ananatis* and *Pantoea stewartii* subsp. *indologenes*. These tailocins are encoded by a locus found within the same approximate genomic context across strains (between *rpoD* and *fadH* and adjacent to a gene for $tRNA_{Met}$) and share a level of divergence similar to other shared genes throughout the genome (~85%–90%). Identification of these loci opens up the possibility that these tailocin molecules could be developed as new prophylactic treatments to prevent infection of crops by *Pantoea* or potentially as a means to limit spread of these strains by various vectors.

ACKNOWLEDGMENTS

This work was supported by a grant from the National Science Foundation (NSF) (IOS 1856556) to D.A.B. and B.H.K.

AUTHOR AFFILIATIONS

[1]Department of Plant Pathology, University of Georgia, Athens, Georgia, USA
[2]School of Animal and Comparative Biomedical Sciences, University of Arizona, Tucson, Arizona, USA
[3]The Plant Center, University of Georgia, Athens, Georgia, USA
[4]Department of Biochemistry, Genetics, and Microbiology, University of Pretoria, Pretoria, South Africa
[5]School of Plant Sciences, University of Arizona, Tucson, Arizona, USA

AUTHOR ORCIDs

Gi Yoon Shin http://orcid.org/0000-0001-8168-5870
David A. Baltrus http://orcid.org/0000-0002-5166-9551

FUNDING

Funder	Grant(s)	Author(s)
National Science Foundation (NSF)	IOS 1856556	David A. Baltrus Brian H. Kvitko

AUTHOR CONTRIBUTIONS

Shaun P. Stice, Conceptualization, Data curation, Formal analysis, Investigation, Methodology | Hsiao-Hsuan Jan, Investigation | Hsiao-Chun Chen, Investigation | Linda Nwosu, Investigation | Gi Yoon Shin, Data curation, Investigation, Writing – review and editing | Savannah Weaver, Investigation | Teresa Coutinho, Investigation, Methodology | Brian H. Kvitko, Conceptualization, Data curation, Formal analysis, Funding acquisition, Investigation, Writing – original draft, Writing – review and editing | David A. Baltrus, Conceptualization, Data curation, Formal analysis, Funding acquisition, Investigation, Methodology, Project administration

ADDITIONAL FILES

The following material is available online.

Supplemental Material

File S1 (AEM00929-23-S0001.txt). Alignment file for sheath protein sequences to recreate phylogenies in manuscript.
File S2 (AEM00929-23-S0002.txt). Alignment file for J plate protein sequences to recreate phylogenies in manuscript.
Figure S1 (AEM00929-23-S0003.tif). A Model For Invertase Activity in the P. stewartii ICMP 10132 Tailocin Locus.

REFERENCES

1. Manesh A, Varghese GM, CENDRIC Investigators and Collaborators. 2021. Rising antimicrobial resistance: an evolving epidemic in a pandemic. Lancet Microbe 2:e419–e420. https://doi.org/10.1016/S2666-5247(21)00173-7
2. Chinemerem Nwobodo D, Ugwu MC, Oliseloke Anie C, Al-Ouqaili MTS, Chinedu Ikem J, Victor Chigozie U, Saki M. 2022. Antibiotic resistance: the challenges and some emerging strategies for tackling a global menace. J Clin Lab Anal 36:e24655. https://doi.org/10.1002/jcla.24655
3. Uddin TM, Chakraborty AJ, Khusro A, Zidan BRM, Mitra S, Emran TB, Dhama K, Ripon MKH, Gajdács M, Sahibzada MUK, Hossain MJ, Koirala N. 2021. Antibiotic resistance in microbes: history, mechanisms, therapeutic strategies and future prospects. J Infect Public Health 14:1750–1766. https://doi.org/10.1016/j.jiph.2021.10.020
4. Kelbrick M, Hesse E, O' Brien S. 2023. Cultivating antimicrobial resistance: how intensive agriculture ploughs the way for antibiotic resistance. Microbiology 169:001384. https://doi.org/10.1099/mic.0.001384
5. Taylor NMI, van Raaij MJ, Leiman PG. 2018. Contractile injection systems of bacteriophages and related systems. Mol Microbiol 108:6–15. https://doi.org/10.1111/mmi.13921
6. Ghequire MGK, De Mot R. 2015. The tailocin tale: peeling off phage tails. Trends Microbiol 23:587–590. https://doi.org/10.1016/j.tim.2015.07.011
7. Scholl D. 2017. Phage tail-like bacteriocins. Annu Rev Virol 4:453–467. https://doi.org/10.1146/annurev-virology-101416-041632
8. Baltrus DA, Clark M, Hockett KL, Mollico M, Smith C, Weaver S. 2022. Prophylactic application of tailocins prevents infection by *Pseudomonas syringae*. Phytopathology 112:561–566. https://doi.org/10.1094/PHYTO-06-21-0269-R
9. Príncipe A, Fernandez M, Torasso M, Godino A, Fischer S. 2018. Effectiveness of tailocins produced by *Pseudomonas fluorescens* SF4c in controlling the bacterial-spot disease in tomatoes caused by *Xanthomonas vesicatoria*. Microbiol Res 212–213:94–102. https://doi.org/10.1016/j.micres.2018.05.010
10. Patz S, Becker Y, Richert-Pöggeler KR, Berger B, Ruppel S, Huson DH, Becker M. 2019. Phage tail-like particles are versatile bacterial nanomachines - a mini-review. J Adv Res 19:75–84. https://doi.org/10.1016/j.jare.2019.04.003
11. Ge P, Scholl D, Prokhorov NS, Avaylon J, Shneider MM, Browning C, Buth SA, Plattner M, Chakraborty U, Ding K, Leiman PG, Miller JF, Zhou ZH. 2020. Action of a minimal contractile bactericidal nanomachine. Nature 580:658–662. https://doi.org/10.1038/s41586-020-2186-z
12. Heiman CM, Maurhofer M, Calderon S, Dupasquier M, Marquis J, Keel C, Vacheron J. 2022. Pivotal role of O-antigenic polysaccharide display in the sensitivity against phage tail-like particles in environmental *Pseudomonas* kin competition. ISME J 16:1683–1693. https://doi.org/10.1038/s41396-022-01217-8
13. Köhler T, Donner V, van Delden C. 2010. Lipopolysaccharide as shield and receptor for R-pyocin-mediated killing in *Pseudomonas aeruginosa*. J Bacteriol 192:1921–1928. https://doi.org/10.1128/JB.01459-09
14. Baltrus DA, Clark M, Smith C, Hockett KL. 2019. Localized recombination drives diversification of killing spectra for phage-derived syringacins. ISME J 13:237–249. https://doi.org/10.1038/s41396-018-0261-3
15. Jayaraman J, Jones WT, Harvey D, Hemara LM, McCann HC, Yoon M, Warring SL, Fineran PC, Mesarich CH, Templeton MD. 2020. Variation at the common polysaccharide antigen locus drives lipopolysaccharide diversity within the *Pseudomonas syringae* species complex. Environ Microbiol 22:5356–5372. https://doi.org/10.1111/1462-2920.15250
16. Baltrus DA, Weaver S, Krings L, Nguyen AE. 2023. Genomic correlates of tailocin sensitivity in *Pseudomonas syringae*. bioRxiv. https://doi.org/10.1101/2023.04.24.538177
17. Carim S, Azadeh AL, Kazakov AE, Price MN, Walian PJ, Lui LM, Nielsen TN, Chakraborty R, Deutschbauer AM, Mutalik VK, Arkin AP. 2021. Systematic discovery of pseudomonad genetic factors involved in sensitivity to tailocins. ISME J 15:2289–2305. https://doi.org/10.1038/s41396-021-00921-1

18. Weaver SL, Zhu L, Ravishankar S, Clark M, Baltrus DA. 2022. Interspecies killing activity of *Pseudomonas syringae* tailocins. bioRxiv 168. https://doi.org/10.1099/mic.0.001258
19. Yao GW, Duarte I, Le TT, Carmody L, LiPuma JJ, Young R, Gonzalez CF. 2017. A broad-host-range tailocin from Burkholderia cenocepacia. Appl Environ Microbiol 83:e03414-16. https://doi.org/10.1128/AEM.03414-16
20. Ghequire MGK, Dillen Y, Lambrichts I, Proost P, Wattiez R, De Mot R. 2015. Different ancestries of R tailocins in rhizospheric *Pseudomonas* isolates. Genome Biol Evol 7:2810–2828. https://doi.org/10.1093/gbe/evv184
21. Nakayama K, Takashima K, Ishihara H, Shinomiya T, Kageyama M, Kanaya S, Ohnishi M, Murata T, Mori H, Hayashi T. 2000. The R-type pyocin of *Pseudomonas aeruginosa* is related to P2 phage, and the F-type is related to lambda phage. Mol Microbiol 38:213–231. https://doi.org/10.1046/j.1365-2958.2000.02135.x
22. Hockett KL, Renner T, Baltrus DA. 2015. Independent co-option of a tailed bacteriophage into a killing complex in *Pseudomonas*. mBio 6:e00452. https://doi.org/10.1128/mBio.00452-15
23. Gebhart D, Williams SR, Bishop-Lilly KA, Govoni GR, Willner KM, Butani A, Sozhamannan S, Martin D, Fortier L-C, Scholl D. 2012. Novel high-molecular-weight, R-type bacteriocins of *Clostridium* difficile. J Bacteriol 194:6240–6247. https://doi.org/10.1128/JB.01272-12
24. Coetzee HL, De Klerk HC, Coetzee JN, Smit JA. 1968. Bacteriophage-tail-like particles associated with intra-species killing of Proteus vulgaris. J Gen Virol 2:29–36. https://doi.org/10.1099/0022-1317-2-1-29
25. Strauch E, Kaspar H, Schaudinn C, Dersch P, Madela K, Gewinner C, Hertwig S, Wecke J, Appel B. 2001. Characterization of enterocoliticin, a phage tail-like bacteriocin, and its effect on pathogenic Yersinia enterocolitica strains. Appl Environ Microbiol 67:5634–5642. https://doi.org/10.1128/AEM.67.12.5634-5642.2001
26. Smarda J, Benada O. 2005. Phage tail-like (high-molecular-weight) bacteriocins of Budvicia aquatica and Pragia fontium (Enterobacteriaceae). Appl Environ Microbiol 71:8970–8973. https://doi.org/10.1128/AEM.71.12.8970-8973.2005
27. Nguyen HA, Tomita T, Hirota M, Kaneko J, Hayashi T, Kamio Y. 2001. DNA inversion in the tail fiber gene alters the host range specificity of carotovoricin Er, a phage-tail-like bacteriocin of phytopathogenic *Erwinia carotovora* subsp. carotovora Er. J Bacteriol 183:6274–6281. https://doi.org/10.1128/JB.183.21.6274-6281.2001
28. Gitaitis RD, Gay JD. 1997. First report of a leaf blight, seed stalk rot, and bulb decay of onion by Pantoea ananas in Georgia. Plant Dis 81:1096. https://doi.org/10.1094/PDIS.1997.81.9.1096C
29. Wells JM. 1987. Isolation and characterization of strains of *Erwinia ananas* from honeydew melons. Phytopathology 77:511. https://doi.org/10.1094/Phyto-77-511
30. Stice SP, Stumpf SD, Gitaitis RD, Kvitko BH, Dutta B. 2018. *Pantoea ananatis* genetic diversity analysis reveals limited genomic diversity as well as accessory genes correlated with onion pathogenicity. Front Microbiol 9:184. https://doi.org/10.3389/fmicb.2018.00184
31. Pal N, Block CC, Gardner CAC. 2019. A real-time PCR differentiating *Pantoea stewartii* subsp.*stewartii* from *P. stewartii* subsp. indologenes in corn seed. Plant Dis 103:1474–1486. https://doi.org/10.1094/PDIS-06-18-0936-RE
32. Stice SP, Shin GY, De Armas S, Koirala S, Galván GA, Siri MI, Severns PM, Coutinho T, Dutta B, Kvitko BH. 2021. The distribution of onion virulence gene clusters among *Pantoea* spp. Front Plant Sci 12:643787. https://doi.org/10.3389/fpls.2021.643787
33. Kvitko BH, Bruckbauer S, Prucha J, McMillan I, Breland EJ, Lehman S, Mladinich K, Choi K-H, Karkhoff-Schweizer R, Schweizer HP. 2012. A simple method for construction of pir+ enterobacterial hosts for maintenance of R6K replicon plasmids. BMC Res Notes 5:157. https://doi.org/10.1186/1756-0500-5-157
34. Stice S.P, Thao KK, Khang CH, Baltrus DA, Dutta B, Kvitko BH. 2020. Thiosulfinate tolerance is a virulence strategy of an atypical bacterial pathogen of onion. Curr Biol 30:3130–3140. https://doi.org/10.1016/j.cub.2020.05.092
35. Hockett KL, Baltrus DA. 2017. Use of the soft-agar overlay technique to screen for bacterially produced inhibitory compounds. J Vis Exp, no. 119:55064. https://doi.org/10.3791/55064
36. Arndt D, Grant JR, Marcu A, Sajed T, Pon A, Liang Y, Wishart DS. 2016. PHASTER: a better, faster version of the PHAST phage search tool. Nucleic Acids Res 44:W16–W21. https://doi.org/10.1093/nar/gkw387
37. Sievers F, Higgins DG. 2018. Clustal omega for making accurate alignments of many protein sequences. Protein Sci 27:135–145. https://doi.org/10.1002/pro.3290
38. Darriba D, Posada D, Kozlov AM, Stamatakis A, Morel B, Flouri T. 2020. Modeltest-NG: a new and scalable tool for the selection of DNA and protein evolutionary models. Mol Biol Evol 37:291–294. https://doi.org/10.1093/molbev/msz189
39. Kozlov AM, Darriba D, Flouri T, Morel B, Stamatakis A. 2019. Raxml-NG: a fast, scalable and user-friendly tool for maximum likelihood phylogenetic inference. Bioinformatics 35:4453–4455. https://doi.org/10.1093/bioinformatics/btz305
40. Wei Z-L, Yang F, Li B, Hou P, Kong W-W, Wang J, Chen Y, Jiang Y-L, Zhou C-Z. 2022. Structural insights into the chaperone-assisted assembly of a simplified tail fiber of the myocyanophage Pam3. Viruses 14:2260. https://doi.org/10.3390/v14102260
41. North OI, Davidson AR. 2021. Phage proteins required for tail fiber assembly also bind specifically to the surface of host bacterial strains. J Bacteriol 203:e00406-20. https://doi.org/10.1128/JB.00406-20
42. Thaler JO, Baghdiguian S, Boemare N. 1995. Purification and characterization of xenorhabdicin, a phage tail-like bacteriocin, from the lysogenic strain F1 of Xenorhabdus nematophilus. Appl Environ Microbiol 61:2049–2052. https://doi.org/10.1128/aem.61.5.2049-2052.1995
43. Jabrane A, Sabri A, Compère P, Jacques P, Vandenberghe I, Van Beeumen J, Thonart P. 2002. Characterization of serracin P, a phage-tail-like bacteriocin, and its activity against *Erwinia amylovora*, the fire blight pathogen. Appl Environ Microbiol 68:5704–5710. https://doi.org/10.1128/AEM.68.11.5704-5710.2002
44. Gaudriault S, Thaler J-O, Duchaud E, Kunst F, Boemare N, Givaudan A. 2004. Identification of a P2-related prophage remnant locus of *Photorhabdus luminescens* encoding an R-type phage tail-like particle. FEMS Microbiol Lett 233:223–231. https://doi.org/10.1016/j.femsle.2004.02.009
45. Yamada K, Hirota M, Niimi Y, Nguyen HA, Takahara Y, Kamio Y, Kaneko J. 2006. Nucleotide sequences and organization of the genes for carotovoricin (Ctv) from *Erwinia carotovora* indicate that Ctv evolved from the same ancestor as *Salmonella typhi* prophage. Biosci Biotechnol Biochem 70:2236–2247. https://doi.org/10.1271/bbb.60177
46. Zink R, Loessner MJ, Scherer S. 1995. Characterization of cryptic prophages (monocins) in Listeria and sequence analysis of a holin/endolysin gene. Microbiology 141 (Pt 10):2577–2584. https://doi.org/10.1099/13500872-141-10-2577
47. Matsui H, Sano Y, Ishihara H, Shinomiya T. 1993. Regulation of pyocin genes in *Pseudomonas aeruginosa* by positive (prtN) and negative (prtR) regulatory genes. J Bacteriol 175:1257–1263. https://doi.org/10.1128/jb.175.5.1257-1263.1993
48. Wu W, Jin S. 2005. PtrB of *Pseudomonas aeruginosa* suppresses the type III secretion system under the stress of DNA damage. J Bacteriol 187:6058–6068. https://doi.org/10.1128/JB.187.17.6058-6068.2005
49. Granato ET, Foster KR. 2020. The evolution of mass cell suicide in bacterial warfare. Curr Biol 30:2836–2843. https://doi.org/10.1016/j.cub.2020.05.007
50. Carter ME, Smith A, Baltrus DA, Kvitko BH. 2022. Convergent gene expression patterns during compatible interactions between two *Pseudomonas syringae* pathovars and a common host (*Nicotiana benthamiana*). https://doi.org/10.1101/2022.06.26.497614